

Analysis of Optimization of Blank Holding Force In Deep Drawing By Using LS DYNA

Gyadari Ramesh, Dr.G.Chandra Mohan Reddy

Department of Mechanical Engineering, Osmania University, Hyderabad-500085.

ABSTRACT

Sheet metal forming problems are typical in nature since they involve geometry, boundary and material non-linearity. Cup drawings involves many parameters like punch and die radius, clearance, lubrication, blank holding force and its trajectories etc. So designing the tools for cup drawing involves a lot of trial and error procedure. To reduce number of costly trial error steps, the process can be simulated by using finite element packages. Even the finite element package gives an approximation towards the solution. The experimentation is inevitable. The aim is to study analysis of optimization of blank holding force developed for cup drawing operation by using explicit finite element package LS DYNA. One of the basic problems in deep drawing is wrinkling. Wrinkling can be avoided by using blank holding force. But higher the blank holding force (BHF), higher is the frictional force, so more will be tensile stresses in cup wall there by promote tearing failure at the punch corner. Hence BHF needs to optimized so as to prevent the wrinkling and at the same time to prevent tearing failure. In this work die design is done for a cup of 30mm diameter and deep with 1 mm thickness. For the same blank holding force is calculated from the empirical formula. The same is simulated on an explicit finite element package LS DYNA. By an iterative procedure the optimum blank holding force is obtained and presented. B H F in deep drawing is an essential parameter to be determined optimally to avoid formation of wrinkles. It is also necessary to at the same time to determine the force in drawing operation and failure of the cup. Higher the B H F, higher is the frictional forces between the blank and blank holder, so higher the loads required for drawing operation and higher the strains developed in the cup walls between the die and punch, thereby reducing thickness of the section. In this thesis optimum blank holding force has been found out by checking the condition of nonformation of wrinkles at different coefficient of friction at (0.045, 0.06, 0.1, 0.13, and 0.15) and at different die radius (2, 3, 4, 5,6mm) and the values of blank holding force has been taken where no wrinkles has been formed for different coefficient of friction and for different die radius and the graphs are plotted and the results are studied. h-Method is used for mesh convergence stability of

max vonmises stress is taken as a parameter to check the convergence.

Keywords – Deep Drawing by Using LS DYNA, Blank Holding and blank holding force (BHF).

I. INTRODUCTION

Sheet metal forming is one of the most widely used manufacturing processes for the fabrication of a wide range of products in many industries. The reason behind sheet metal forming gaining a lot of attention in modern technology is due to the ease with which metal may be formed into useful shapes by plastic deformation processes in which the volume and mass of the metal are conserved and metal is displaced from one location to another. Deep drawing is one of the extensively used sheet metal forming processes in the industries to have mass production of cup shaped components in a very short time. In deep drawing, a flat blank of sheet metal is shaped by the action of a punch forcing the metal into a die cavity Sheet metal forming is one of the most common manufacturing processes to plastically deform a material into a desired shape. Products include hundreds of automotive components, beverage cans, consumer appliances, submarine hulls, and air craft frames. Based on the geometry, the volume and the material, sheet metal forming can be divided into various categories such as stamping, deep drawing, stretch forming, rubber forming, and super plastic forming. Among these, Stamping and deep drawing are the most common operations.

Deep drawing products in modern industries usually have a complicated shape, so these have to undergo several successive operations to obtain a final desired shape. Trimming of the flange is one of those operations and that is used to remove the ears i.e. to have uniform shape of the flange on all the sides of the final product. These are formed due to uneven metal flow in different directions, which is primarily due to the presence of the planar anisotropy in the sheet.

The main concern of the deep drawing industry is to optimize the process parameters in order to get a complete deep drawn product with least effects and high limiting drawing ratio. In order to achieve this optimization objective a large number of solution runs need to be performed in order to search for the optimum solution. Furthermore, the quality of

the products can be increased. With reference to an economical success it is very important to put better and cheaper products faster on the market than other competitor's. A substantial aid for this is the numerical simulation. Costs and time for tool adapting could play an outstanding roll. Furthermore, changes in design while fabricating a prototype are usual. By means of numerical simulation, potential forming problems can be recognized during fabricating a first tool. Despite many advantages of the numerical simulation, it must be said, that there are costs for hardware, software, training and for the simulation itself. However, it is an effective means for making forming processes and new products cheaper. Tool loads can be computed and overloads can be predicted by means of FEM, which is very difficult in practical experiments.

The depth of draw may be shallow, moderate or deep. If the depth of the formed cup is more than its diameter, the process is called Deep Drawing. Parts of various geometric and sizes are made by drawing operation, two extreme example being bottle caps, automobiles panels etc. the simplest example is the drawing of a flat bottom cylindrical cup.

In the drawing of a cylindrical cup, a round sheet metal blank, is placed over a circular die opening and is held in place with a blank holder. The punch travels downward and forces the blank into the die cavity, forming a cup. The important variables in deep drawing are the properties of sheet metal, the ratio of blank diameter to punch diameter, the clearance between the punch and die, the punch corner radius and die corner radius, the blank holder force, friction and lubrication. The forces occurring during drawing are bending at the radii, friction between blank holder and sheet metal, die and sheet metal, punch and sheet metal and compression at flange area or extremity of cup. Usually Drawing is a process of forming a flat, pre-cut, metal blank into a hollow shape, either cylindrical or box-shaped, by pressing it into a die cavity without excessive wrinkling, thinning, or fracturing. Typical parts produced by drawing include beverage cans, containers of all shapes and sizes, and automobile and aircraft panels. Deep drawing process is influenced by some parameters like residual stresses, Blank holding force etc.

Residual stresses also play a very important role in how a formed part in a deep drawn cup. These stresses can become so large in a deep drawn cup that cracks are formed in the cup wall. These residual stresses can be removed by annealing the cup right after the deep drawing. However in most cases it is desire to avoid the annealing process. This process increases the production costs, and can lead to an inexpedient production flow and can give problems with regard to maintaining close tolerances due to distortion during annealing process.

B H F is an important parameter in deep drawing process. It is used to suppress the formation of wrinkles that can appear in the flange of the drawn part. When increasing the B H F, stress normal to the thickness increases which restrains any formation of wrinkles.

However, the large value of the B H F will cause fracture at the cup wall and punch profile. So, the B H F must be set to a value that avoids both process limits of wrinkling and fracture. Avoid wrinkling and tearing such that at each punch travel (L), the following relations must be satisfied:

$FBH > F$ wrinkling and $FBH < F$ Tearing

A given technical problem must be expressed by physical terms so that it can be formulated mathematically, what means modeling. The model should reflect the reality as exactly as possible. However, it should also be as simple as possible. Furthermore, the model must be described this way that it can be implemented in computers. Numerical problems like divisions by extremely low numbers or poor convergences of iterations, respectively, have to be mastered or to be avoided. Trial runs of the computational simulations and a subsequent check of the results by comparison with reality or physical experiments are a must. A special attention has to be directed to the boundary and initial conditions during modeling because they have a decisive influence on the extent of the model as well as on its reliability. If the results do not coincide with reality or with the expectations close to reality, the model must be checked and possibly modified, whereby it will become bigger and more complicated.

II. HEADINGS

I. INTRODUCTION

II. LITERATURE SURVEY

2.1. Sheet Metal Forming

2.1.1. Objective

2.1.2. Types of Forming

2.1.3. Theory of sheet metal drawing operation.

2.1.4. Reducing severity of draw

2.2. Deep Drawing

2.3. Wrinkling & Tearing

2.4. Blank Holding Force

III. MATHEMATICAL FORMULATION

3.1. Co-rotational coordinates

3.2. Velocity-Strain Displacement Relations

3.3. Stress Resultants and Nodal Forces

3.4. Material properties

3.4.1. Power Law Isotropic Plasticity

3.4.2. Rigid Material

IV. Design Calculations

4.1. Blank diameter

4.2. Allowances for Trimming

- 4.3. Percentage reduction
- 4.4. Thickness to diameter ratio
- 4.5. Drawing Force

V. FINITE ELEMENT SIMULATIONS

- 5.1. Selection of optimum mesh size for the blank
- 5.2. Selecting optimum Blank Holding Force at different Coefficient of Friction
- 5.3. Selecting optimum Blank Holding Force at different Die Radius
- 5.4. Variations of vonmises stresses with blank holding force at different Coefficient of Friction
- 5.5. Variation of plastic strain with Blank Holding Force at different Coefficient of Friction
- 5.6. Variation of Vonmises stresses with Blank Holding Force at different Die Radius
- 5.7. Variation of Plastic strain with Blank Holding Force at different Die Radius

VI.SIMULATION RESULTS

VI.CONCLUSION

6.1 Conclusion

REFERENCES

II. OBJECTIVE

The main objective of the proposed research is to find the optimal blank holding force that is to be used in the deep drawing process to produce a cup of required shape and size without wrinkles at different coefficient of friction and at different die radius. For general deep drawing operations, most people define the optimal blank shape as that blank profile which can be deformed into a cup with either a uniform flange profile or uniform rim height i.e. cup free from ears. However it is not easy to find an optimal blank holding force because of complexity of deformation behavior and there are couple of process parameters like die radius, punch radius, punch speed, blank holder force and amount of friction which affects the result of the process i.e. tearing, wrinkling, spring back and surface conditions such as earing. Even a slight variation in one of these parameters can result in defects. Until now, the optimal blank holding force along with the input of optimal process parameters is performed by a trial and error method based on the expertise of the engineer. But recently, in order to address the change of demand from mass production to batch production for higher quality products in ever shorter time, this experimental trial and error technique has turned out to be very expensive and

time consuming. Therefore, numerical simulations of sheet metal forming processes based on the finite element method (FEM) represent a powerful tool for prediction of forming processes.

III. LITERATURE SURVEY:

3.1 Sheet Metal Forming:

In metal forming, a piece of material is plastically deformed between tools to obtain the desired product. A special class of metal forming concerns the case where the thickness of the piece of material is small compared to the other dimensions, i.e. sheet metal forming. Sheet metal forming is a widely used production process: in 1998, 265 million tons of steel sheet and 9 million tons of aluminum sheet was produced worldwide which was approximately 35% of the total steel and aluminum production [Langerak, 1999a][1]. Sheet metal forming is characterized by a stress state in which the component normal to the sheet plane is generally much smaller than the stresses in the sheet plane. A commonly used sheet metal forming process is the deep drawing process. The principle of deep drawing is schematically represented in Figure 3.1.

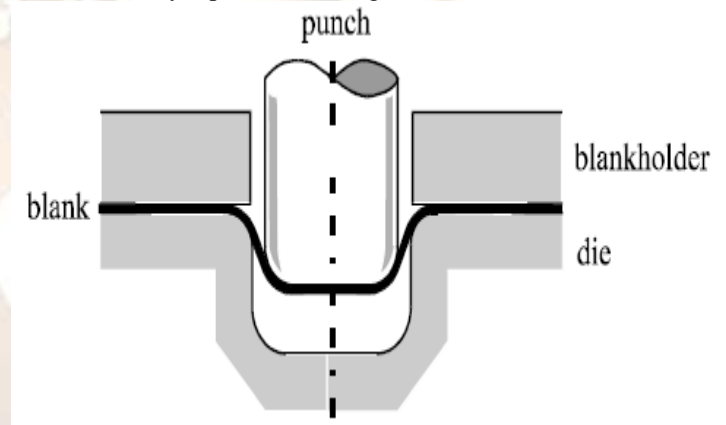


Fig. 3.1 Schematic of deep drawing process

Haar and carleer [2] mentioned the material flow into the die cavity is controlled by the blank holder; a restraining force is created by friction between the tools and the blank. The friction between the tools and the blank is influenced by the blank holder force, lubrication or by coatings on the blank or tools. The work as described in this thesis is implemented in the implicit finite element code DiekA. The finite element code DiekA developed at the University of Twente, is a multi-purpose package which is able to simulate various forming processes such as rolling, deep drawing, extrusion, cutting and slitting. The deep drawing part of this code was developed in close cooperation with Hoogovens Research and Development, a part of the Corus Group PLC since October 6, 1999. The development of the deep drawing part of DiekA was started in 1987. In 1992, Vreede[3] presented deep drawing simulation results of axi-symmetric products,

rectangular products and a simple automotive product, making use of a 3-node triangular element based on membrane theory (i.e. only incorporating stretching energy) [Vreede, 1992]. The material behavior was described by rigid plastic constitutive relations and the planar isotropic Hill yield criterion. The contact behavior was described by special contact elements and Coulomb friction. Finally, the tools were numerically described by a collection of measurement points or by elements. In 1992, the work of Vreede was continued by Carleer. The new developments were focused on improving the existing code in order to better satisfy the requirements for industrial application. In the subsequent five years, the following improvements were implemented [Carleer, 1997]: two new 3-node triangular element types, i.e. an element based on Kirchhoff theory (incorporates membrane and bending stresses) and an element based on Mindlin theory (incorporates membrane, bending and shear stresses). The anisotropic behavior of the material was taken into account by implementing the anisotropic Hill'48 yield criterion and the Vegter[4] yield criterion based on multiaxial stress states [Vegter, 1999]. An elastoplastic constitutive relation was implemented in order to predict the springback behavior after deep drawing. The contact description was improved by a fast contact search algorithm and a more sophisticated friction model. Finally, an equivalent draw bead model was developed to efficiently incorporate draw beads in a finite element simulation. Sheet metal forming is characterized by large relative displacements between the sheet and the tooling, spatial and temporal strain variations in the part and complex boundary conditions. Robust and accurate analysis is needed to simulate forming process and defects, with the ultimate goal to eliminate costly die-tryouts, particularly when introducing new materials and processes. Finite element models must be computationally efficient for practical use with today's computers and those in foreseeable future. Wang and budiasky[5] introduced the membrane element formulation based on a theory of shells presented by budiasky[6]. When compared to large strain, large displacement, and elastoplastic shell formulations {7-9}, membrane formulations have been reported to be 5 times faster [10-12]. Earlier research in our group showed of 5x to 20x for shell simulations versus membrane ones. 3-D continuums are seldom applied to general forming because of limited computation time [10-11]. The computational efficiency of membrane elements, make them attractive for arbitrary 3D geometries, but they fail to produce a convergent solution for bending-dominated forming problems, or to reproduce bending effects such as flange/ wall wrinkling or spring back.

Hybrid methods based on empirical results introducing bending effects into membrane sheet

forming programs have been proposed. Stoughton [10] reduced the terms of tangent stiffness matrix using a draw bead model of Wang [14]. Good results were reported for R/t ratios ranging from 3.1 to 18.4 with minimal increase in computer time, approximately 6%. Pourboghart and chandorkar [15] used the contact conditions, stress and strain states and curvatures of the tooling to adjust the membrane solution (after computation), and to calculate spring back and side wall curl. Although both approaches were computationally efficient, they have proven difficult to generalize to arbitrary geometries. For linear-elastic problems, corrections to the membrane residual vector and corresponding stiffness matrix have been formulated [16-119]. Inter element bending was evaluated from the relative rotations of adjacent two elements; the bending stiffness is being represented by torsional springs of a specified stiffness.

Similar approaches have been developed for non linear sheet forming problems, where the sheet is discretized into two superimposed meshes accounting for bending and stretching [20-26]. Keum [20] introduced this concept without the mechanical formulation for FE implementation. Huh et al. [21-23] derived a family of 'Bending Energy Augmented Membrane' (BEAM) elements with rotational springs at nodes or at element edges. The bending stiffness of this matrix for these elements were assumed as constant during a time step and updated at the end of time step. Six-noded patches of four constants strain triangular elements have been used to compute the inter-element bending forces for dynamic explicit programs based on an elastic constitutive law [24] and elastic plastic constitutive law [25].

3.1.1 TYPES OF FORMING

Many forming operations are complex, but all consists of combinations or sequences of the basic forming operations bending, stretching and drawing.

3.1.1.1 Bending:

Bending is the metal working process by which a straight length is transformed into a curved length it is a very common forming process for changing sheet and plate into channels, drums tanks etc. during the bending operations, the outer surface of the material is in tension and the inside surface in compression. The strain in the bent material is increases with decreasing radius of curvature. The stretching of the bend causes the neutral axis of the section to move towards the inner surface. In most cases, the distance of the neutral axis from the inside of the bend is $0.3t$ to $0.5t$, where "t" is the thickness of the part.

3.1.1.2 Stretch forming:

Stretch forming is the process of forming by the application of primarily tensile forces in such a way as to stretch the material over a tool or form block. Stretching is caused by tensile stresses in

excess of the yield stress. When they are applied in perpendicular directions in the plane of the sheet, these courses produce biaxial stretching. When the perpendicular forces are equally balanced biaxial stretching occurs. Much higher levels of deformation as measured by an increase in area can be reached in balanced biaxial stretching than in any other forming mode. Many forming operations involve stretching of some means within the stamping. Automotive outer body panels are typical examples of parts formed primarily by stretching. Parts with regions containing domes (microwave reflectors), ribs and embossments also involve stretching.

3.1.2 Theory of sheet metal drawing operation

Many irregular shaped parts are drawn, and the theories of metal flow in these parts are complicated. The drawing of cups is the simplest drawing operation and more easily illustrated. Therefore the remaining discussion refers to the operation known as cupping. The blank required for cupping is round. An analysis should be made of what happens as the punch and die first starts to draw the blank. The blank edge is forced down to a smaller circumference; such a reduction means that a compressive force is being applied to the metal.

3.1.2.1 Metal flow:

Drawing operation consists of metal flow rather than metal movement. These terms were described in the theory of forming sheet metal. During cupping, the metal flows into the cup shape, the metal follows itself into the cup shape. There is no movement of metal through space as there is during a forming operation, the metal flows through the opening provided by the clearance between the punch and die and blank holder. Since the punch exerts the force on the cup bottom to cause the drawing action, considerable stretching of metal occurs in the cup side wall near the cup bottom. Fig 3.2

Fig 3.2 Forces during Cupping

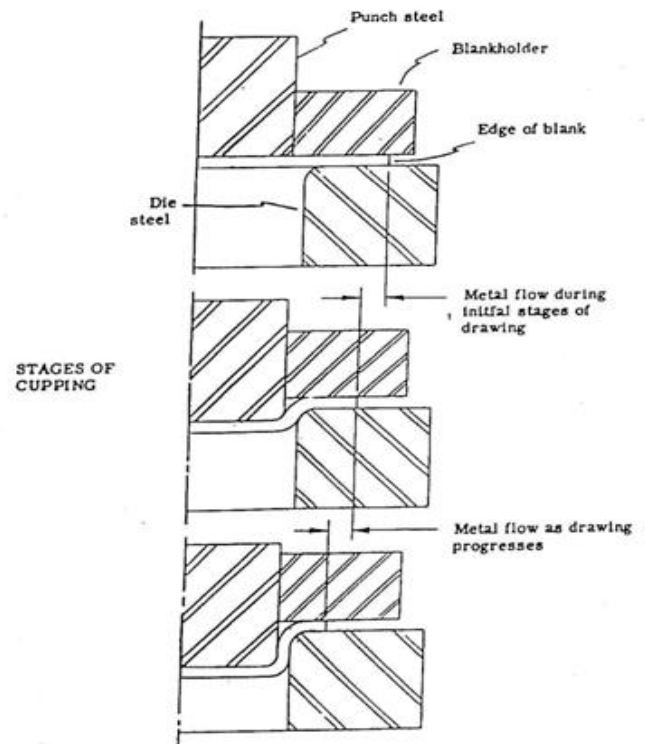


Fig 3.3 Metal flow During Cupping

shows metal flow in cupping die. Figure 3.3 shows the forces involved on the outer edge of the blank, this metal tends to thicken. The thinning and thickening of metal in the cupping operation also may be referred to as metal flow.

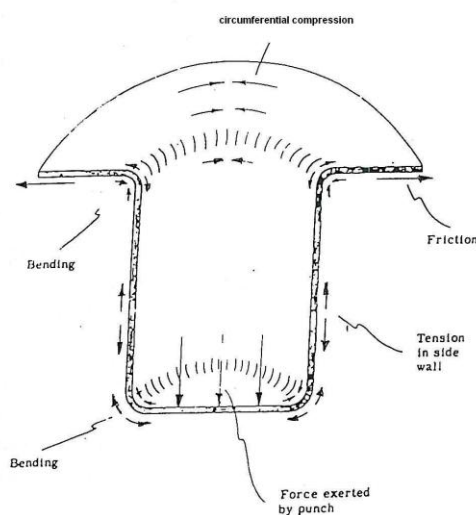
1.2.2 Forces during drawing:

The forces occurring during drawing are:

1. Bending at the radius
2. Friction between
 - a. Blank holder and sheet metal
 - b. Die and sheet metal
 - c. Punch and sheet metal
3. Compression at flange area or extremity of cup.

The punch exerts a force on the cup bottom of sufficient magnitude to overcome the sliding and stationary friction, to bend force it at the radii and to compress the metal at the cup extremity. Therefore the punch force is the sum of the other three. The punch force is the applied force and the other three are totaled to obtain the equal and opposite reaction force.

Wrinkles are formed due to improper design of the die. The die has to given a taper in order to increasing the load force. This may also happen due to the improper lubrication. The force is transmitted by the cup side wall. The wall is placed under tension at a point near the cup bottom. If the punch force or the total of the other three forces exceeds the ultimate tensile strength of the metal, the wall will break. The final analysis of force is as follows:



Friction + compression + bending = punch force severity.

The punch force must be less than the ultimate strength of the metal or failure will occur.

3.1.3 Characteristic cupping force curve:

The curve representing the force required during cupping reveals many characteristics of drawing. The maximum force occurs at the first instant of cupping. Therefore, cupping consists of high instantaneous force, which immediately reduces after metal flow has been started. The base of the cupping force curve represents the depth of the cup. The graph shown in figure 3.4 between punch force and punch stroke for drawing operation gives the total punch force, friction, ideal deformation and ironing.

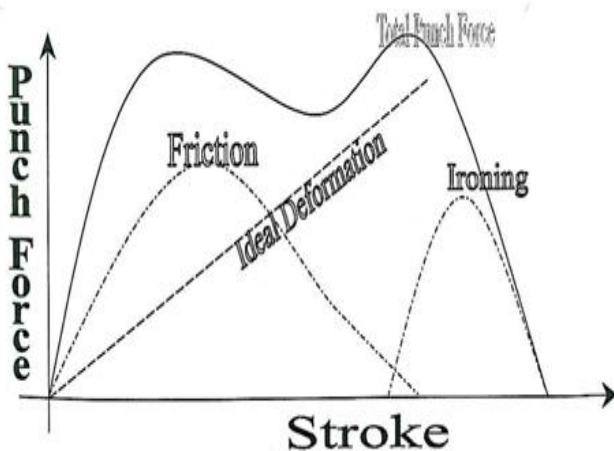


Fig 3.4 Punch force vs. punch stroke for drawing operation

The main conclusion that can be made from the curve is that the initial contact of the punch steel with the metal blank is the point of severest stress or strain. If wrinkles occur, they start while this high force is applied. If the cup breaks, failure occurs while this high force is applied. Once metal flow has started and the force is reduced, the chances of wrinkles or cup breaking are limited. If cup failure occurs after this point, the failure can usually be attributed to inclusions or defects in the sheet metal. As long as blank size and punch diameter are being used. Whether or not a flange is left on the cup has no effect on the severity of the operation. This condition is illustrated in figure 3.5. The measure of the severity of drawn is found by comparing the punch diameter. For irregular shaped drawing, a comparison of the blank area will the initial contact area of the punch would be an indicator of

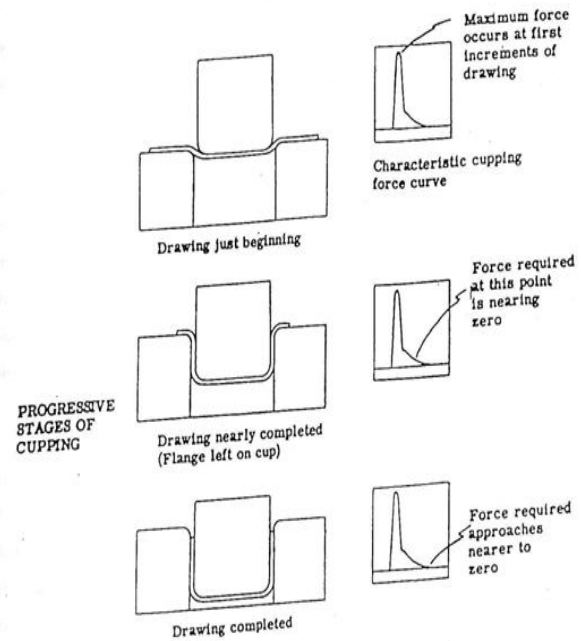


Fig 3.5 Severity of drawing

Drawing severity is determined by the relationship between the punch diameter and blank diameter. The larger the difference in diameter the greater the severity in drawing. Greater severity means there is more tendencies for wrinkling and tearing. When the punch diameter and blank diameter are constant, the severity of drawing is not reduced because a flange is left on the cup. If no flange is left on the cup, the severity of draw is not appreciably increased. This is because of small difference in force requirements as illustrated above.

3.1.4 Reducing severity of draw:

Several methods may be employed to reduce the severity of draw. Any method that increases the relative punch contact area will reduce the severity. It is assumed that a drawing lubricant or compound is being used to permit free metal flow. The blank holding pressure must also be correct.

The severity of the draw may be reducing by the following methods:

1. Increase draw radii
2. Change blank holding surface to an angle
3. Provide lead in or chamfer on die
4. Pre fold the blank with the blank holder wrap
5. Pre fold the blank before placing it in the draw die
6. Use redrawing to obtain final size

3.1.4.1 Draw radii:

If possible the radius on the punch is made the same as the part print radius. The same is true of the radius on the die. Many times, however, these radii are too small and increase the severity of the drawing operation. A small radius restricts the flow

of metal over the radius. When metal flow is retarded in such manner, a higher force is required to start the flow. This higher force is converted to greater tension on the cup side wall and may cause failure. This failure may occur before the cup is completely drawn.

Therefore to reduce the severity of drawing and reduce metal failure, the radius on the punch and die is increased. Because more metal flow occurs over the die radius this is the most critical radius.

3.1.4.2 Redrawing:

When simpler methods fail, the redraw operation is used to reduce severity. The diameter of the draw punch is increased to reduce the draw severity. The difference between the blank and punch diameter is reducing. The draw punch diameter is increased to a point where successful draws can be made. This means that the cup produced is too large in diameter and too short in height when compared to the part print. Therefore, secondary operation called 'redraws' are necessary to reduce the diameter to part print specification. One or more draws may require. Drawing, then, is converting cups from flat blanks. Redrawing is reducing a cup or drawn part to a smaller diameter with resulting increase in height. After drawing, the metal is in a work hardened state. Therefore redrawing must be consecutively less severe in reduction to prevent failure of the metal. Often it is necessary to anneal parts before or between redrawing operations.

3.1.4.3 Restricting metal flow:

On irregular shaped blanks and panels it is often desirable to restrict the flow of metal into the die. Metal flow must be restricted when an access of metal is flowing into an area. Adding draw beads or splines on the blank holding surface restricts flow. When metal flow must be stopped altogether, the lock bean may be employed. The bead restricts metal flow by causing the metal to bend and unbend. Varying the bead contour and height may alter the degree of bead restriction. The bead leaves a depression in the scrap area of the metal, which is subsequently trimmed off. Decreasing the draw radius can also restrict metal flow and using a horizontal blank holding surface can also restricts metal flow. Serrations in the blank holding surface will also restrict metal flow. Varying lubricant consistency on using no lubricant at all may also control metal flow.

3.1.4.4 Trimming:

Because the blank must be gripped to prevent wrinkles and because the metal is often scratched or scored when moving under the blank holder, excess metal is provided in the blank, this excess score metal is cut away by the trimming operation. Bed depressions are also contained in this scrap.

3.2 Deep drawing

In a deep drawing process, the blank is deformed into its final desired shape by displacing a punch into a die and deforming the central region of the blank. The punch force deforms the blank by straining it against a constraint which is created by clamping the blank between a die and a blank holder along its periphery. The force used to clamp the blank between the die and blank holder is called the blank holder force ~BHF!. The blank holder force can be varied to achieve many desired objectives, from preventing the occurrence of tearing or wrinkling, and therefore, increasing the draw depth [25–27], to controlling springback [28,29]. The blank holder force can also be varied spatially, by employing segmented binders, flexible binders and local adaptive controllers [30–34]. Variation of blank holder force ~BHF! can be determined *a-priori*, as applied in an open-loop manner, or by using a feedback loop, as a result of feedback control. One of the first examples of work done on blank holder force control was that of Hardt and Lee [35]. Using the general concept of a safe region between wrinkling and tearing, they proposed two closed-loop control strategies for a conical cup forming. The first method was designed to maintain a constant blank holder displacement, allowing a limited amount of flange wrinkling. The blank holder force was kept at the minimum necessary to prevent buckling in the unsupported region and also to prevent tearing. The second approach tried to control the binder force by regulating the volume of material entering the die cavity, through a generalized thickness parameter (t^*). The conclusion drawn was that the strategies did not appreciably increase the maximum cup height, but did significantly reduce the sensitivity of this maximum value to changes in the blank holder control variable. Kergen and Jodogne [36,37] performed studies aimed at determining minimum BHF curve trajectories for various steels, based on a wrinkle detection system that measured the distance between the die and the blank holder in a cylindrical cup forming. The authors found that the measured BHF trajectories and the minimum BHF obtained from experiments varied significantly with variations in the types and properties of steels being tested. Hirose et al. [38] showed the success of an increasing linear combination BHF pattern in preventing the formation of wrinkles in an automobile panel. The authors further concluded that if a decreasing, linear combination BHF trajectory is used, body wrinkles are not suppressed.

Other researchers have reported favorable results obtained with decreasing BHF profiles. Kirii et al. [39], who also tested different linear combination patterns of BHF in panel formation, concluded that a decreasing BHF scheme was the optimum approach. Ahmetoglu et al. [40] obtained a different set of results. The authors employed

computer simulation in the drawing of a round cup, in which three variables ~punch force, radial stress and thickness strain! were used to control the blank holder force during simulation. The authors smoothed the results into a single decreasing BHF trajectory, which was then used to draw a cylindrical steel cup. This decreasing trajectory was used to successfully increase the draw depth over the case of a constant binder force. Ahmetoglu et al. [41] further examined decreasing binder force trajectories with regard to the deep drawing of rectangular parts from aluminum alloy 2008-T4. Their experiments indicated that a decreasing binder force significantly reduced the amplitude of wrinkles, while avoiding the fracture associated with high BHF values. The work of Sim and Boyce [42]. The authors performed axisymmetric cup forming process simulations based on the tangential force and normalized average thickness trajectories. These models yielded numerical results for BHF trajectories that were later employed to increase the height to which cups could be drawn. Cao and Boyce [27] built upon this work to develop a novel approach to determine a variable BHF trajectory. The authors performed finite element simulations with PI control of the blank holder force. They were able to calculate a BHF trajectory having a combined upward and downward portion that showed a 16% increase in forming height over the results obtained by the best constant binder force case. Recently, experiments by Siegert and Ziegler [43] have shown that the onset of wrinkling in a blank drawn with a pulsating BHF occurs at a displacement similar to that obtained under a constant BHF equal to the maximum force of pulsation. The reduction in the friction force achieved due to the pulse allows more material flow to take place, thus reducing the chances of tearing. Hsu et al. [44] proposed an approach for modeling sheet metal forming for process controller design. They developed a process model for U-channel forming, i.e., a mathematical relationship between the blank holder force and the punch force was determined and validated experimentally. Characterization of model uncertainty due to blank size, sheet thickness, material properties and tooling shape was also studied. The process model was shown to be effective in describing the forming process. Blank holder force variation has also been used to effectively control spring back in sheet metal forming. Using the concept of intermediate restraining, Cao et al. [28] used a neural network to determine a stepped binder force trajectory that was used to minimize springback and also obtain consistent results in channel forming, despite the presence of material variations and different lubricants. The approach was shown to be robust and applicable to a wide range of materials and process conditions. Liu et al. [29] used a similar approach in the forming of U-shaped parts and

concluded that forming quality was improved when a variable binder force trajectory was used.

The use of segmented tooling and flexible binders is an area of sheet metal forming that has also been gaining prominence in recent years. The advantages of spatial variation of blank holder force have been cited in several research endeavors. One of the first examples of segmented binder tooling can be found in Siegert et al. [30]. The authors discussed a deep drawing apparatus developed at the Institute of Metal Forming Technology in which the lower binder is composed of eight individual segments, four corner segments and four straight segments. Each of these segments is powered by its own separate hydraulic cylinder. This allows an optimal blank holder force to be applied to individual regions of the blank. Thus, the blank holder force can be varied spatially in such a manner that individual segments of the binder can apply optimal values of blank holder force as desired. Neugebauer et al. [31] performed studies using flexible binders and multiple draw pins. Their experimental set up consisted of an asymmetric part and a binder which had 12 draw pins distributed evenly along its periphery. The draw pins could be used to apply different values of binder force. They studied four cases, a rigid binder ~80 mm thick! with a uniform pin force, a rigid binder with a non-uniform pin force, a flexible binder ~30 mm thick! with a uniform pin force and a flexible binder with a nonuniform pin force. Although no major difference was observed in the two cases where a rigid binder was used, the case of a flexible binder with constant pin force increased the maximum achievable drawing depth from 70 mm to 90 mm. In the case of a flexible binder with non-uniform pin force, draw depths up to 110 mm were achieved. Doege et al. [32] proposed an innovative concept in which the blank holder is designed as an elastically deformable thin steel plate. The authors used FEM analysis to determine the plate thickness and the location of support elements holding the binder. They performed experiments at various binder force values to estimate a "safe working area." The authors were able to show that the safe working area for a part is larger with a pliable blank holder and it moves towards higher blank holder force values. Furthermore, it was shown that the distribution of pressure on the blank was more uniform, thus giving rise to improved part quality. Kinsey et al. [33] proposed a novel method of forming tailor welded blanks that incorporated a segmented die with local adaptive controllers. The local adaptive controllers consisted of hydraulic cylinders positioned in such a manner as to create an additional constraint within the forming area. The position of this constraint is selected so as to minimize the weld line movement and therefore reduce the strain developed in the thinner material. Experiments performed on an asymmetric part

showed that this method of forming helped increase the draw depth by 20% over the conventional case.

The deep drawing process is applied with the intention of manufacturing a product with a desired shape and no failures. The tools, the blank and the process parameters define deep drawing final product shape. An incorrect design of the tools and blank shape or an incorrect choice of material and process parameters can yield a product with a deviating shape or with failures.

In the deep drawing the most common defects are presented in figure 3.6 [45]. In figure 3.6, the notations are: 1. flange undulation; 2. side undulation; 3. piece wrinkling; 4. circular traces; 5. scratches; 6. orange peel; 7. Luders bands; 8. cracking of piece flange or piece bottom; 9. edges cracking; 10.- disalignment; 11. Contour disalignment; 12. festoons; 13. delaminations; 14. edge festoons [1]. Some of these are the result of the dies (5, 9, 10, 14), another are due to friction conditions (1, 4, 13), others are as the result of the material composition (6, 13) and of the mechanical properties of the material (1, 2, 3, 6, 7, 8, 11) and others are as the result of the piece form (12, 14). For deep drawing by stretching only defects of types 3, 6 and 8 are common [46].

The forming limit curves, FLDs, is one of the method in examining the failure potential, which include a good representation of material's stretch ability and the easiness when used for trouble shooting.

In the design of deep drawing processes, many process parameters, e.g. die geometry, initial blank shape, blank holding force, and lubrication, need to be determined. It is critical to the industry that these design variables are optimized for one particular forming process.

The design process has traditionally relied on experience and intuition accompanied in many cases by physical trial and error approach. With the development of computer technology, numerical simulations using, for example, incremental finite element methods (FEM) have been developed.

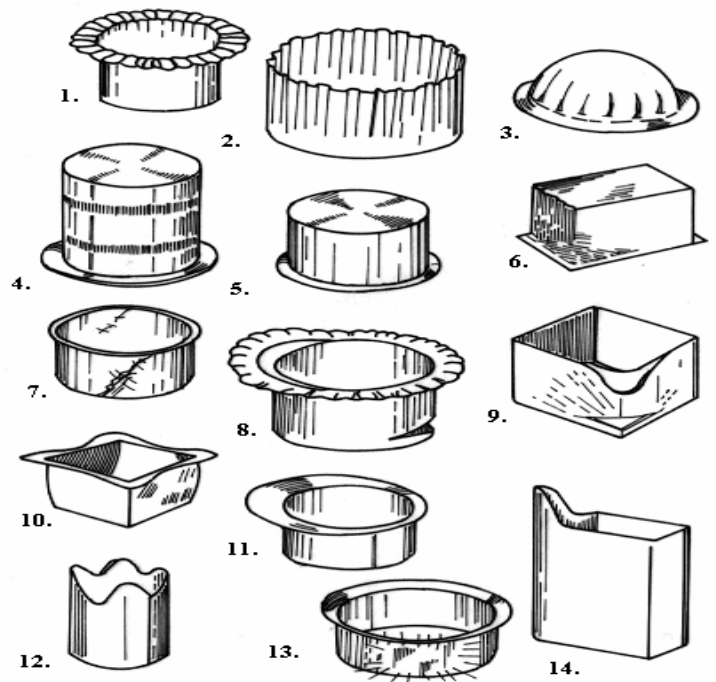


Fig. 3.6. - Types of defects in deep drawing

However, the majority of the applications using finite element methods has been deterministic, in which a set of design parameters is given and simulation results are interpreted by users. Additional simulations need to be performed if the results are not satisfactory. The determination of those design parameters is again mainly based on users' experience and interpretation. Such design process usually requires enormous amount of time and cost to determine the optimal process parameters. Since metal forming processes are generally highly non-linear and history dependent, many researchers have used the direct differentiation method for the calculation of sensitivity [46,52]. Badrinarayanan and Zabarar [46; 47] calculated the differentiation terms directly from the weak form of equilibrium equations and demonstrated the approach on determining a preform shape of an upsetting problem and a die profile of an extrusion problem. Alternatively, the differentiation terms can be derived from the finite element discretized weak form as described in Chenot and co-workers [47,48]. They calculated a preform shape of an upsetting problem and tool shapes of a two-step forging problem. Zhao and colleagues [49,50] developed a similar optimization scheme to that of Chenot and co-workers. They focused on the optimal design of die shapes of performs rather than that of preform shapes. Kleiber et al. [51,52] derived sensitivity equations by both the direct differentiation method and the adjoint variable method. Joun and Hwang [53] used the adjoint variable method to optimize the die profile of a three-dimensional steady-state extrusion problem. Most sensitivity analyses for incremental FEM have been

applied to simple two-dimensional problems such as upsetting, forging, and extrusion. However, there is very little practical application to sheet metal forming processes and many difficulties still remain in the implementation of sensitivity analysis to practical and complex bulk forming problems.

3.3 Wrinkling & Tearing

Wrinkling is one of the major defects in sheet metal forming, together with tearing, spring-back and other geometric and surface defects. Many research efforts have been dedicated to predict the occurrence, the location, and the shape of the wrinkles as evident in the review articles, which emphasized the work initiated from Hill's general theory of uniqueness and bifurcation. Here the importances of material models on the prediction results have been discussed. In most of the finite element analyses (FEA), accumulated computational error can be treated as an artificial imperfection in the system to initiate the wrinkling, but the necessary magnitude to initiate wrinkling is problem dependent. This nature determines the uncertainties associated with the FEA in practical applications. Cao [54] proposed a stress-based wrinkling predictor. Cao et al. [54] developed a multi-scale approach with mesh-free adaptivity to simulate the wrinkling behavior of sheet metals, while using the stress-based predictor to generate the desired enrichment function. This method is now able to capture the wrinkling and post-buckling behavior in an elastic plate and wedge strip examples. With all the numerical work, it is necessary to have well-controlled experiments to verify the numerical approaches. The experimental work can be divided into two categories. The first category includes simple tests of special specimens designed for simulating the basic mechanism. Sheet buckling/wrinkling is one of the critical issues not only in sheet metal forming itself but also in the numerical simulation of this process. Buckling can limit the ability to stretch sheet metal during processing and adversely affect final part appearance and functionality; severe wrinkling may damage or even destroy dies. Due to the complexity of buckling, much research on this topic has been carried out case by case for a given process by experiment. Yoshida et al. [55] investigated the material resistance to wrinkling by stretching a square sheet along one of its diagonals. A deep drawing of a conical cup and square cup was analyzed by Senior, Jalkh et al. [54]. Zhang and Yu [56] conducted research on drawing of elastic-plastic circular plates using a spherical punch. Besides experimental work, analytical investigation on the plastic wrinkling initiated from the study on columns by Shanley [57], followed by the study on plate and shells by Tvergaard [58] and Needleman, V.Tvergaard also proposed a similar concept [59]. General analytical study of plastic wrinkling began with Hill's 1958 bifurcation and uniqueness theory

and was detailed for plates and shell in Hutchinson (1974)[60]. The theory is essentially an Eigen value of the bifurcation function. Hutchinson and Neale (1985)[61] later extended Hutchinson's 1974 work to the conditions needed for the onset of wrinkling in doubly curved sheet metal without lateral constraint. They found that wrinkling is most likely a local instability problem depending on the local curvature and local stress states. This finding applies to plates and shells whose top and bottom surfaces are free of contact. The problem differs slightly when we consider the effect of a lateral constraint (constraint normal to the plane of the sheet) on buckling in the case of sheet metal forming, lateral constraints are present in the form of binder/sheet/die or die/sheet/die interactions where the sheet is constrained to some extent between a binder and a die or matching dies via force controlled or displacement controlled condition. Our previous experimental and numerical work (Jalkh et al., 1993[62]) showed that wrinkling behavior depends upon the pressure applied normal to the sheet by the binder, as well as the local stress states and curvature. The closest analytical solution for this situation is given by Triantafyllidis and Needleman (1980)[63]. They applied the bifurcation theory to an annular plate subjected to axisymmetric radial tension along its inner edge. By resting the annular plate on a continuous linear elastic foundation, they treated the binder as a deformable binder and obtained the effect of binder stiffness on a critical buckling stress and the wave number. Also they assume small strain deformation. Unfortunately, a direct comparison between the analytical results and experimental results were given.

3.4 Blank holding force

By understanding the mechanics of metal deformation in sheet metal forming and having condensed in numerical simulations, the next logical step is to design the Process using numerical simulations. Very early attempts utilized the slip line theory [64], upper bound analysis, and lower bound analysis. An inverse method using deformation theory was developed for designing the initial blank shape in [65]. Based on the minimum plastic work principle, Chung and Richmond [66] proposed an ideal forming theory to design the optimal blank shape and forming procedures [67]. With the development of data acquisition systems and computer hardware, the concept of variable binder force was introduced by Hirose et al. [68]. More recently, the ability to change the binder force during the forming process is no longer limited to a research apparatus stamping plants. However, most of the work found in the literature utilized a force trajectory generated by a trial-and-error approach. Using a control element in their FEM model, Cao and Boyce [69] monitored the tendency of wrinkling and tearing

and thereby, designed a single variable binder force trajectory for a conical cup forming using numerical simulation. This trajectory was implemented in experiments and led to a 16% increase in the Ultimate forming height of the cup over the traditional processes.

Fenn and Hardt [70] developed a real-time closed-loop control system to alter the binder force during the forming process using the actual punch force or material draw-in as inputs. They obtained consistent forming heights despite the presence of variations in the lubricant, blank location and initial binder force. This approach was adopted successfully by Jalkh et al. [71] for aluminum cup forming.

Spring back can be reduced through modifications to the forming process. Several researchers have proposed to use a stepped binder force trajectory to accomplish this objective (Ayres[72], 1984; Hishida and Wagoner[73], 1993; Sunseri[74] et al., 1996). A stepped binder force trajectory is an instantaneous jump from a low binder force (LBF) value to a high binder force (HBF) at a specified percentage of the total punch displacement (PD%) . Sunseri et al. (1996) but is also available in commercial stamping presses, which can be found in all the major automotive companies' investigated springback in the Aluminum channel forming process. Their work was conducted through experiments and simulations at specific values for process and material parameters.

For the constant binder force (CBF) cases there exists an optimal CBF which results in a max cup height with out wrinkling or tearing failure. However, CBF experiments do not necessarily optimize material flow trajectories for forming without failure. Hirose[75] et al. (1990) examined binder force trajectories containing step changes while forming full scale automobile panels .All trajectories that did succeed were those that started at low binder forces and then increased during the later stage of the process. The results obtained were successful but were obtained by intensive trail and error. Much recent work on sheet metal has focused on designing variable binder force (VBF) histories with majority papers reports a success in experimental trail and error approach.

Another promising method to determine the optimal binder force trajectory in the forward mode was presented in Cao and Boyce [76] for a given initial blank geometry and tooling geometry. A user-defined element serves the purpose of closed-loop control in the FEM simulation. This Element senses the current wrinkling and tearing tendencies and alters the binder force so that no Excessive wrinkles are present. The optimal binder force history was determined in one run of the FEM simulation.

IV. MATHEMATICAL FORMULATION

In the present formulation the BELYTISCHKO Lin Stay shell element from LS DYNA IS USED The element has 5 through the thickness integration points and it requires 725 mathematical operations.

BELYTISCHKO shell element is based on a combined rotational and strain formulation the efficiency of the element is obtained from the mathematical simplifications that result from these two kinematical assumptions. The co rotational portion of the formulation avoids the complexity of non linear mechanics by embedding a coordinate system in the element. The choice of velocity strain, or rate of deformation, in the formulation facilitates the constitutive evaluations, since the conjugate stress is more familiar Cauchy stress.

4.1 Co rotational coordinates

The mid surface of quadrilateral shell element , or reference surface, is defined by the location of elements four corner nodes . An embedded element coordinate system as shown in figure that deforms with the element is defined in terms of this local coordinates. Then the procedure for constructing the co rotationalco ordinate system begins by calculating a unit vector nrmal to the main diagonal of the element

$$\hat{e}_3 = \frac{s_3}{\|s_3\|} \quad (4.1a)$$

$$\|s_3\| = \sqrt{[s_{31}^2 + s_{32}^2 + s_{33}^2]} \quad (4.1b)$$

$$s_3 = r_{31} \hat{X} r_{42} \quad (4.1c)$$

Where the super script caret (.) is used to indicatethe local(element) coordinate system.

It is desired to establish the local x axis \hat{x} approximately along the element edge between nodes 1 and 2. This definiton is convenient for interpreting the element stresses which are defined in local \hat{x} - \hat{y} coordinate system.the procedure for constructing this unit vector is to define a vector s_1 that is nearly parallel to the vector r_{21} .

$$s_1 = r_{21} - (r_{21} \cdot \hat{e}_3) \hat{e}_3 \quad (4.2a)$$

$$\hat{e}_1 = \frac{s_1}{\|s_{11}\|} \quad (4.2b)$$

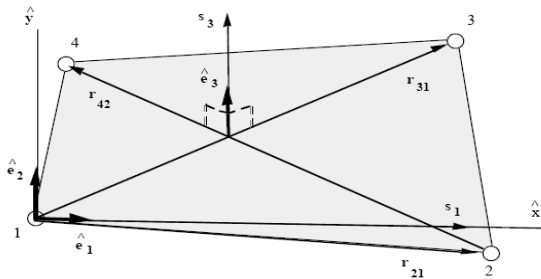


Fig 4.1 construction of element coordinate system

The remaining unit vector is obtained from the vector cross product.

$$\hat{e}_2 = \hat{e}_3 \times \hat{e}_1 \quad (4.3)$$

If the four nodes of the element are coplanar, then the unit vectors \hat{e}_1 and \hat{e}_2 are tangent to the midplane of

the shell and \hat{e}_3 is in the fiber direction. As the element deforms, an angle may develop between the

actual fiber direction and the unit normal \hat{e}_3 . The magnitude of this angle may be characterized as

$$|\hat{e}_3 \cdot \hat{f} - 1| < \delta \quad (4.4)$$

Where \hat{f} is the unit vector in the fiber direction and the magnitude of δ depends on the magnitude of the strains. According to Belytschko et al, for most engineering applications acceptable values of δ are on the order of 10^{-2} and if the condition presented in Equation (4.4) is met, then the difference between

the rotation of the co-rotational coordinates \hat{e} and the material rotation should be small. The global components of this co-rotational triad define a transformation matrix between the global and local element coordinate systems. This transformation operates on vectors with global components $A = (A_x + A_y + A_z)$ and element coordinate components $A = (A_x + A_y + A_z)$ and is defined as;

$$\begin{aligned} \{A\} &= \begin{Bmatrix} A_x \\ A_y \\ A_z \end{Bmatrix} = \begin{bmatrix} e_{1x} & e_{2x} & e_{3x} \\ e_{1y} & e_{2y} & e_{3y} \\ e_{1z} & e_{2z} & e_{3z} \end{bmatrix} \begin{Bmatrix} \hat{A}_x \\ \hat{A}_y \\ \hat{A}_z \end{Bmatrix} = \\ [\mu] \{ \hat{A} \} &= [q]^T \{ \hat{A} \} \end{aligned} \quad (4.5a)$$

Where e_{ix}, e_{iy}, e_{iz} the global components of the element are coordinate unit vectors. The inverse transformation is defined by the matrix transpose, i.e.

$$\{ \hat{A} \} = [\mu]^T \{ A \} \quad (4.5b)$$

4.2 Velocity-Strain Displacement Relations

The above small rotation condition s , Equation (4.4), does not restrict the magnitude of the element's rigid body rotations. Rather the restriction is placed on the out-of-plane deformations, and thus on the element strain. Consistent with this restriction on the magnitude of the strains, the velocity-strain displacement relations used in the Belytschko-Lin-Stay shall are also restricted to small strains.

As in the Hughes -Liu shell element, the displacement of any point in the shell is partitioned into a mid surface displacement (nodal translations) and a displacement associated with rotations of the element's fibers (nodal rotations). The Belytschko-Lin-Tsay shell element uses the Mindlin (1951) theory of plates and shells to partition the velocity of any point in the shell as

$$v = v^m - z \hat{e}_3 \times \theta \quad (4.6)$$

Where V^m is the velocity of the mid-surface, θ is

the angular velocity vector, and z is the distance along the fiber direction (thickness) of the shell element. The corresponding co-rotational components of the velocity strain (rate of deformation) are given by

$$\hat{d}_{ij} = \frac{1}{2} \left(\frac{\partial \hat{v}_i}{\partial x_j} + \frac{\partial \hat{v}_j}{\partial x_i} \right) \quad (4.7)$$

Substitution of Equation (3.6) into the above yields the following velocity-strain relations.

$$\hat{d}_x = \frac{\partial \hat{d}_x^m}{\partial x} + z \frac{\partial \hat{\theta}_y}{\partial x} \quad (4.8a)$$

$$\hat{d}_y = \frac{\partial \hat{v}_y^m}{\partial y} - z \frac{\partial \hat{\theta}_x}{\partial y} \quad (4.8b)$$

$$2 \hat{d}_{xy} = \frac{\partial \hat{v}_x^m}{\partial y} + \frac{\partial \hat{v}_y^m}{\partial x} + z \left(\frac{\partial \hat{\theta}_y}{\partial y} - \frac{\partial \hat{\theta}_x}{\partial x} \right) \quad (4.8c)$$

$$2 \hat{d}_{xy} = \frac{\partial \hat{v}_z^m}{\partial y} - \hat{\theta}_x \quad (4.8d)$$

$$2 \hat{d}_{xz} = \frac{\partial \hat{v}_z^m}{\partial x} - \hat{\theta}_y \quad (4.8e)$$

The above velocity-strain relations need to be evaluated at the quadrature points within the Shell.

Standard bilinear nodal interpolation is used to define the mid surface velocity, angular Velocity, and the element's coordinates (isoperimetric representation). These interpolations relations are given by

$$V^m = N_I(\xi, \eta)V_I \quad (4.9a)$$

$$\theta^m = N_I(\xi, \eta)\theta_I \quad (4.9b)$$

$$X^m = N_I(\xi, \eta)X_I \quad (4.9c)$$

Where the subscript I is summed over all the element's nodes and the nodal velocities are obtained by differentiating the nodal coordinates with respect

to time, i.e. $v_I = \dot{x}_I$. The bilinear shape functions are

$$N_1 = \frac{1}{4}(1 + \xi)(1 + \eta) \quad (4.10a)$$

$$N_2 = \frac{1}{4}(1 + \xi)(1 - \eta) \quad (4.10b)$$

$$N_3 = \frac{1}{4}(1 - \xi)(1 + \eta) \quad (4.10c)$$

$$N_4 = \frac{1}{4}(1 - \xi)(1 - \eta) \quad (4.10d)$$

The velocity strains at the center of the element, i.e., at $\xi = 0$ and $\eta = 0$ are obtained by substitution of the above relations into the previously defined velocity-strain displacement relations, Equations (4.8a) and (4.8e). After some algebra, this yields

$$\hat{d}_x = B_{1I} \hat{v}_{xI} + \hat{z} B_{1I} \hat{\theta}_{yI} \quad (4.11a)$$

$$\hat{d}_y = B_{2I} \hat{v}_{yI} - \hat{z} B_{2I} \hat{\theta}_{xI} \quad (4.11b)$$

$$2\hat{d}_{xy} = B_{2I} \hat{v}_{xI} + B_{1I} \hat{v}_{yI} + \hat{z} (B_{2I} \hat{\theta}_{yI} - B_{1I} \hat{\theta}_{xI}) \quad (4.11c)$$

$$2\hat{d}_{xz} = B_{1I} \hat{v}_{zI} + N_I \hat{\theta}_{yI} \quad (4.11d)$$

$$2\hat{d}_{yz} = B_{2I} \hat{v}_{zI} + N_I \hat{\theta}_{xI} \quad (4.11e)$$

Where,

$$B_{1I} = \frac{\partial N_I}{\partial x} \quad (4.12a)$$

$$B_{2I} = \frac{\partial N_I}{\partial y} \quad (4.12b)$$

The shape function derivative B_{aI} are also evaluated at the center of the element i.e. at $\xi = 0$ and $\eta = 0$

3.3. Stress Resultants and Nodal Forces.

After suitable constitutive evaluations using the above velocity strains, the resulting stresses are integrated through the thickness of the shell to obtain local resultant forces and moments. The integration formula for the resultants is

$$\hat{f}_{\alpha\beta}^R = \int \hat{\sigma}_{\alpha\beta}^R d\hat{z} \quad (4.13a)$$

$$\hat{m}_{\alpha\beta}^R = -\int \hat{z} \hat{\sigma}_{\alpha\beta}^R d\hat{z} \quad (4.13b)$$

Where the superscript R indicates a resultant force or moment and the Greek subscripts emphasize the limited range of the indices for plane stress plasticity.

The above element –centered force and moment resultants are related to the local nodal forces and moments by invoking the principle of virtual power and performing a one-point quadrature. The relations obtained in this manner are

$$\hat{f}_{xI}^R = A \left(B_{1I} \hat{f}_{xx}^R + B_{2I} \hat{f}_{xy}^R \right) \quad (4.14a)$$

$$\hat{f}_{yI}^R = A \left(B_{2I} \hat{f}_{yy}^R + B_{1I} \hat{f}_{xy}^R \right) \quad (4.14b)$$

$$\hat{f}_{zI}^R = Ak \left(B_{1I} \hat{f}_{xz}^R + B_{2I} \hat{f}_{yz}^R \right) \quad (4.14c)$$

$$\hat{m}_{xI}^R = A \left(B_{2I} \hat{m}_{yy}^R + B_{1I} \hat{m}_{xy}^R - \frac{k}{4} \hat{f}_{yz}^R \right) \quad (4.14d)$$

$$\hat{m}_{yI}^R = -A \left(B_{1I} \hat{m}_{xx}^R + B_{2I} \hat{m}_{xy}^R - \frac{k}{4} \hat{f}_{xz}^R \right) \quad (4.14e)$$

$$\hat{m}_{zI}^R = 0 \quad (4.14f)$$

Where A is the area of the element and k is the shear factor from the Mindlin theory. In the Belytschko-Lin –T say formulation, k is used as a penalty parameter to enforce the Kirchhoff normality condition as the shell becomes thin.

The above local nodal forces and moments are then transformed to the global coordinate system using the transformation relations given previously as Equation (4.5a). The global nodal forces and moments are then appropriately summed over all the nodes and the global equation of motion are solved for the next increment in nodal accelerations.

In the present formulation 2 material properties has been used

1. Power Law Isotropic Plasticity
2. Rigid

1. Power Law Isotropic Plasticity:

Elastoplastic behavior with isotropic hardening is provided by this model. The yield stress, σ_y , is a function of plastic strain and obeys the equation:

$$\sigma_y = \kappa \varepsilon^n = \kappa \left(\varepsilon_{yp} + \bar{\varepsilon}^p \right)^n$$

Where ε_{yp} is the elastic strain to yield and $\bar{\varepsilon}^p$ is the effective plastic strain (logarithmic).

A parameter, SIGY, in the input governs how the strain to yield is identified. If SIGY is set to zero, the strain to yield is found by solving for the intersection of the linearly elastic loading equation with the strain hardening equation:

Where SIGY yield stress

$$\sigma = E \varepsilon$$

$$\sigma = \kappa \varepsilon^n$$

This gives the elastic strain at yield as:

$$\varepsilon_{yp} = \left(\frac{E}{\kappa} \right)^{\left[\frac{1}{n-1} \right]}$$

If SIGY yield is non zero and greater than 0.02 then:

$$\varepsilon_{yp} = \left(\frac{\sigma_y}{\kappa} \right)^{\left[\frac{1}{n} \right]}$$

Strain rate is accounted for using the Cowper and Symonds model which scale the yield stress with the factor

$$1 + \left(\frac{\dot{\varepsilon}}{C} \right)^{1/p}$$

Where $\dot{\varepsilon}$ is the strain rate. A fully viscoplastic formulation is optional with this model which incorporates the Cowper and Symonds formulation within the yield surface. An additional cost is incurred but the improvement in results can be dramatic.

2. Rigid:

The rigid material type provides a convenient way of turning one or more parts comprised of beams, shells, or soled elements into a rigid body. Approximating a deformable body as rigid is a preferred modeling technique in many real world applications.

For example, in sheet metal forming problems the tooling can properly and accurately be treated as rigid. In the design of restraint systems the occupant can, for the purposes of early design studies, also be treated as rigid. Elements which are rigid are bypassed in the element processing and no storage is allocated for storing history variables; consequently, the rigid material type is very cost efficient.

Two unique rigid part ID's may not share common nodes unless they are merged together using

the rigid body merge option. A rigid body may be made up of disjoint finite element meshes, however. LS-DYNA assumes this is the case since this is a common practice in setting up tooling meshes in forming problems.

All elements which reference a given part ID corresponding to the rigid material should be contiguous, but this is not a requirement. If two disjoint groups of elements on opposite side of a model are modeled as rigid, separate part ID's should be created for each of the contiguous element groups if each group is to move independently. This requirement arises from the fact that LS-DYNA internally computes the six rigid body degrees-of-freedom for each rigid body (rigid material or set of merged materials), and if disjoint groups of rigid elements use the same part ID, the disjoint groups will move together as one rigid body.

Inertial properties for rigid materials may be defined in either of two ways. By default, the inertial properties are calculated from the geometry of the constituent elements of the rigid material and the density specified for the part ID. Alternatively, the inertial properties and initial velocities for a rigid body may be directly defined, and this overrides data calculated from the material property definition and nodal initial velocity definitions.

Young's modulus, E, and Poisson's ratio, ν , are used for determining sliding interface parameters if the rigid body interacts in a contact definition. Realistic values for these constants should be defined since unrealistic values may contribute to numerical problem in contact.

V. DESIGN CALCULATIONS

The material properties assigned to blank are shown in table 5.1 and the material properties assigned to remaining are considered as rigid and the schematic view of the model is shown in fig 5.1

Table 5.1: Material properties assigned to blank

S.no	Property	Value
1	Young's modulus (E)	$6.9 \times 10^4 \text{ N/mm}^2$
2	Mass density (ρ)	2.7×10^{-9}
3	Poissons ratio (μ)	0.3
4	Strength coefficient (k)	412.4
5	Hardening exponent (n)	0.255

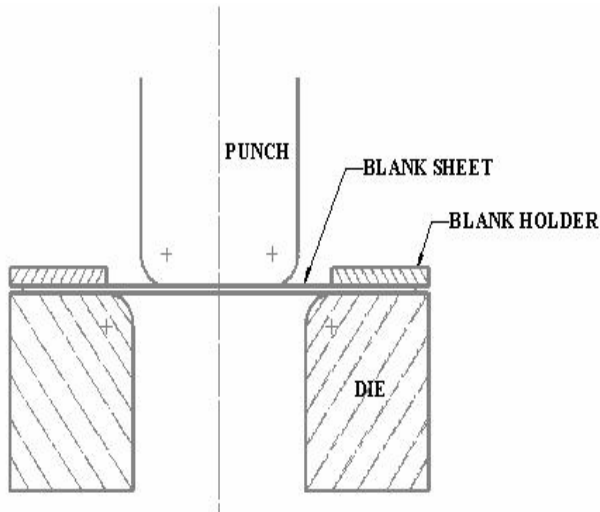


Fig 5.1: Schematic view

The following factors may be calculated with formulas presented here:

- 5.1 Blank diameter
 - a. Prepared formula
 - b. Method for intricate cups
- 5.2 Percent reduction
 - a. Drawing
 - b. Redrawing
- 5.3 drawing force
 - a. Drawing force
 - b. Blank holding force
 - c. Ironing force.

The formulas presented are applicable to the cupping operation only. They may be adjusted, in some cases to approximate forces for irregular shaped panels.

5.1 Blank diameter

The first step in preparing for a cupping operation is find of blank diameter required. If a finished cup is available, it could weight. The blank then has the same weight as the cup. A blank of correct thickness would be cut to the diameter necessary to produce this weight.

Several prepared formulas are available for calculating the blank diameter required for various shapes of cups, as follows:

$$D = \text{blank diameter}$$

$$d = \text{punch diameter}$$

$$h = \text{cup height}$$

$$D = \sqrt{d^2 + 4dh} = 67.08\text{mm}$$

5.2 Allowances for Trimming

As described in the theory of drawing, additional metal must be providing for trimming. Excess metal is needed for gripping. The metal becomes scored and scratched and must be removed. Therefore, after the blank diameter required for the finished cup has been found, the diameter is

increased an amount sufficient for trimming operation. This is called trim allowance.

The larger the cup being drawn, the larger the trim allowances should be. The prediction of blank size for larger cups may be less certain. Approximate trim allowances are as fallows.

Table 5.1: Approximate trim allowances

Cup diameter	Increase in blank diameter
Up to one inch	1/8 inch
From one to two inch	¼ inch
From one to four inch	½ inch
Larger	1 inch

The trim allowance varies with the metal being drawn. Since the trim allowance used is directly related to the scrap percentage produced, care must be taken in setting this allowance.

The final blank diameter is then as fallows:

$$\text{Blank diameter} = \text{Development blank diameter} + \text{Trim allowance}$$

5.3 Percentage reduction:

When the final blank diameter is known, the next step is to determine the percentage of reduction necessary to convert the blank into the desired cup. If the allowed percent reduction for drawing does not produce the final desired cup size, then redraws must be made. The allowable percent of reduction for the redraw determine how many redraws are required. As described in the theory of drawing operation, the severity of cupping is determined by the relationship between the punch steel diameter and blank diameter. The closer these diameters are, the less severe is the operation.

The percentage reduction is an expression of this severity, as fallows:

$$\% \text{ Reduction} = \frac{D-d}{D} \times 100 = 55.27$$

5.4 Thickness to diameter ratio:

Another factor controlling the severity of drawing the ratio of the blank thickness to the blank diameter. When two blanks of equal diameter are to be drawn, the thicker blank can have a higher percent reduction without wrinkling or cup failure. The blank thickness is found as a percent of the blank diameter, as fallows:

$$t = \text{sheet metal thickness}$$

$$D = \text{blank diameter}$$

$$\frac{t}{D} \times 100 = 1.49$$

5.5 Drawing force:

During drawing operation, the side wall is placed tension to cause bending at the radii, overcome friction and compress the metal in the flange. Therefore, the logical way to calculate the drawing force would be to use the tensile strength of the metal.

The force needed to draw a cup is equal to the product of the cross sectional area and the yield strength is in tension of the work material. For a cylindrical cup, the drawing force can be determined by the formula

$$F = \pi d t \sigma_y (D/d - c) \text{ Newtons}$$

Where, c= drawing force constant (varies from 0.52 to 0.7)

$$F = \pi \times 30 \times 1 \times 242 (67.08/30 - 0.7)$$

$$F = 35015.27 \text{ N}$$

$$F = 35.015 \text{ KKN}$$

Therefore Blank holding force = $F/3 = 11.671 \text{ KKN}$

Clearance: Clearance is usually 7 to 14% greater than the sheet thickness i.e. 0.01mm.

VI. FINITE ELEMENT SIMULATIONS

A finite element explicit solver LS Dyna is used for the simulation of effect of various parameters on the optimum blank holding force. In this work the effect of friction coefficient, die radius, clearance, and sheet thickness is studied. The following methodology is applied for the same.

- Tolling design is carried out for the cup of 30mm diameter and 30 mm deep.
- Blank holding force is calculated empirically.
- Modeling is done in CATIA, imported the same to VPG 3.1, a preprocessor for LS DYNA solver.
- In the figures 6(a) we can see the wrinkles formed at different blank holding force but at same coefficient friction. and in fig 6(b) we can see that there are no wrinkles on the flange of cup this cup is taken at calculated blank holding force i.e. 11671
- The finite element model with different mesh sizes are shown in fig 6(c).and the wire frame model is shown in fig 6(d).
- Punch, die and blank holder are selected as rigid materials and material model selected for the blank is as power law plasticity model ($\sigma = K * \epsilon^n$) with the properties shown in table 6.1
- All elements are selected as shell elements. The meshing parameters of the die, punch and blank holder are shown in table 6.2
- Optimum mesh size is found out by considering stability of one of the out put parameters (max von-mise's stress) and the selected mesh size is used for the analysis.

Each parameter is varied keeping other three parameters constant (incase of thickness, instead of clearance, % of clearance is taken as constant) the results are presented and compared.

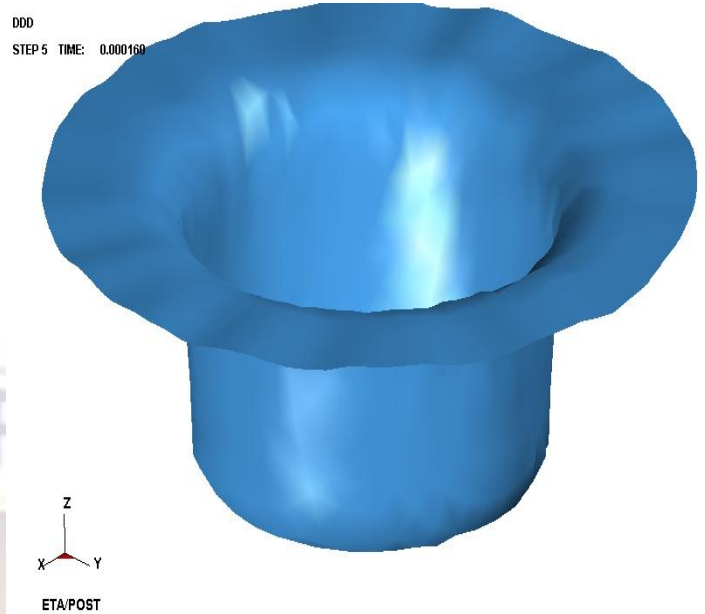


Fig 6(a) Cup with wrinkles at 9500 BHF

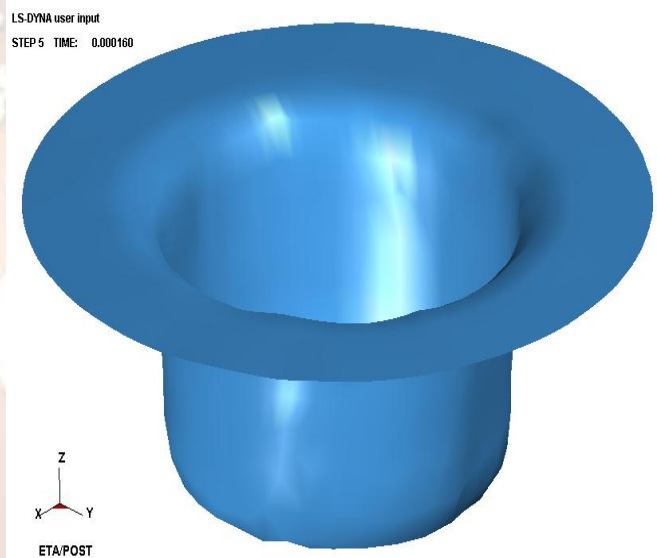


Fig 6(b) Cup without wrinkles at 11671 BHF

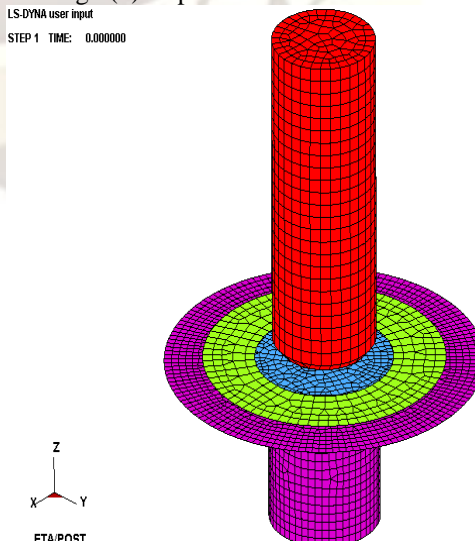


Fig 6(c): Finite element model

LS-DYNA user input
STEP 1 TIME: 0.000000

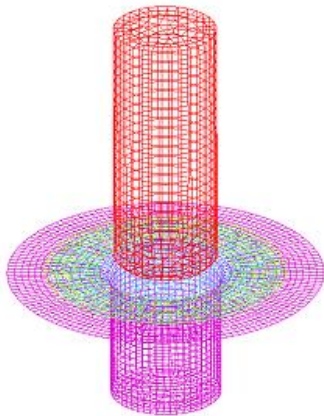
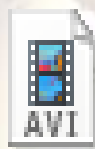


Fig 6(d): Wire frame model

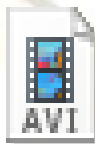
The fig 6(a) is taken at 9500 BHF with 0.15 coefficient friction at 5th time step .and fig 6(b) is taken with calculated BHF (11671) at 0.15 coefficient friction and at same time step i.e.5th those are shown at top left corner of those figures. In fig 6(a) we can se wrinkles where as in case of fig6 (b) there are no formation of wrinkles.



video 1.avi



video 2.avi



video 3.avi

6.1. Selection of optimum mesh size for the blank

Since a numerical solution is an approximate one which may be converged to its true value by refining the mesh or by using higher order elements. In this work the convergence is checked by refining the mesh. It is carried out by studying the stability of one of the out put parameters. The out put parameter chosen here is Max von-mise's stress. Mesh chosen is topology mesh with the max size of 3mm initially.

The simulation is carried out and the max vonmise's stress is noted at each step and plotted in fig 6.1. It is found that the fluctuation is high. Then the mesh size is reduced successively in steps of 0.25 mm and the corresponding values against the punch stroke are plotted (fig 6.1)

Table 6.1: Meshing parameter

		Mesh size			
		3	2.75	2.5	2
	0	0	0	0	0
	0.00004	268.2	269.35	267.01	270.614
	0.00008	345.17	360.864	347.522	340.176
	0.00012	366.45	403.36	381.18	365.91
	0.00016	381.954	401.365	385.82	376.51
	0.0002	386.32	404.288	390.944	385.116
	0.00024	420.434	412.9	420.95	414.522
	0.00028	446.94	452.96	458.6	432.81
	0.00032	459.49	467.75	466.64	455.53
	0.00036	437.199	422.55	475.8	434.17
	0.0004	416.99	468.43	408.97	462.41

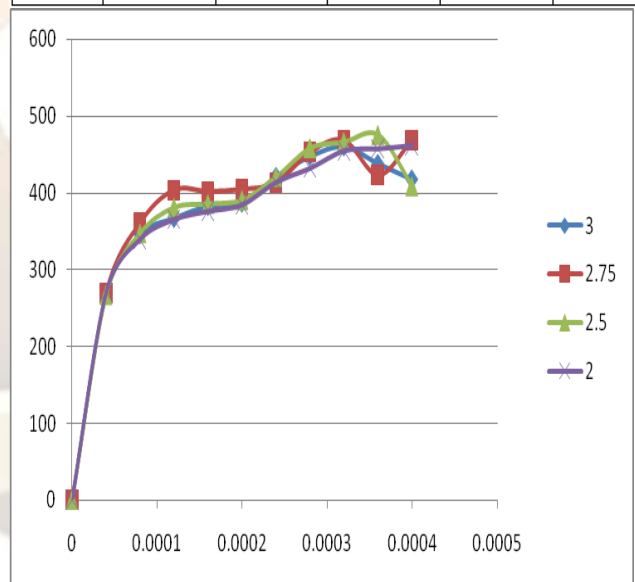


Fig 6.1: Max vonmise's stress v/s punch stroke for various mesh sizes

From the fig 6.1 it is observed that the variation of the max von mise's stress is almost stable for the mesh size of 2mm with the parameters shown in table 6.3

6.2 Selecting optimum blank holding force at different coefficient of friction: In this case checking of wrinkles has been done at

different blank holding force with different coefficient of friction. The blank holding force in table 6.2 is the one where there is no formation of wrinkling at different coefficient of friction.

Table 6.2: Optimum Blank Holding Force Vs Coefficient Of Friction

Coefficient of friction	Blank Holding Force
0.01	11671
0.045	11671
0.06	11500
0.13	11250
0.15	11000

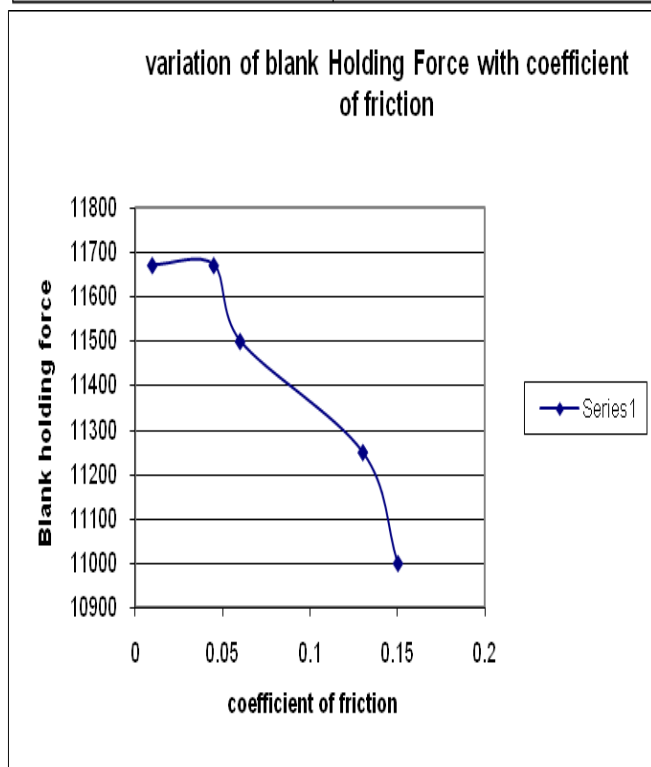


Fig 6.2: variation of blank Holding Force with coefficient of friction

From fig 6.2 it is observed that the Optimum B H F decreases with increase of coefficient of friction. It is found that up to the friction coefficient of 0.05 the decrease is less from 0.06 to 0.13 there is linear variation. Optimum B H F is inversely proportional to coefficient of friction. Either decrease

is linear beyond that the optimum B H F decreases drastically.

6.3 Selecting optimum blank holding force at different die radius

Table 6.3: Optimum Blank Holding Force Vs Different Die Radius

Die radius	B H F
2	11500
3	11000
4	11000
5	11000
6	11000

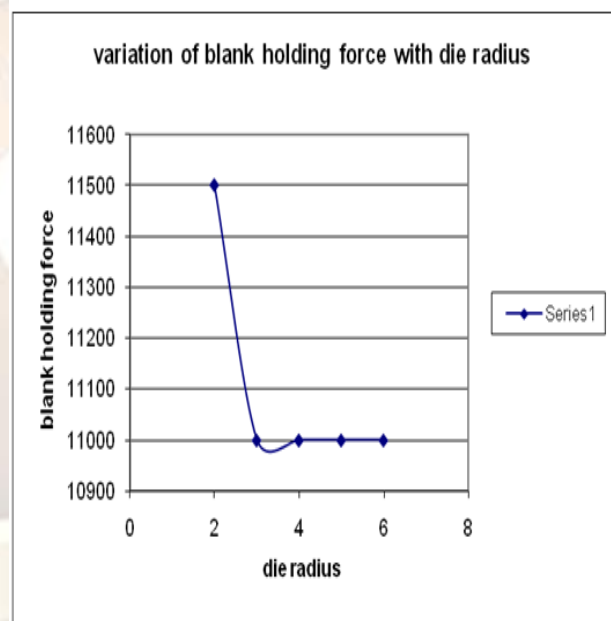


Fig 6.3: variation of blank Holding Force with Die Radius

From fig 6.3 it is evident that the optimum B H F decreases drastically with increase of die radius at smaller die radius. After that it will not affect optimum B H F.

6.4 Variations of vonmises stresses with blank holding force at different coefficient of friction:

Table 6.4: Variations of vonmises stresses with blank holding force at Different coefficient of friction.

		Coefficient of friction				
		0.01	0.045	0.06	0.13	0.15
Blank holding force	10250	3.97E+02	3.88E+02	3.93E+02	3.96E+02	3.88E+02
	10500	3.98E+02	3.95E+02	3.90E+02	3.96E+02	3.95E+02
	10750	3.80E+02	3.93E+02	3.89E+02	4.03E+02	3.93E+02
	11000	3.87E+02	4.13E+02	3.96E+02	4.04E+02	4.13E+02
	11250	4.05E+02	4.04E+02	4.12E+02	4.10E+02	4.04E+02
	11500	3.90E+02	3.89E+02	3.90E+02	4.10E+02	3.89E+02
	11671	3.94E+02	3.86E+02	3.95E+02	4.06E+02	3.86E+02
	11750	3.99E+02	3.96E+02	3.91E+02	4.06E+02	3.96E+02
	12000	3.98E+02	3.94E+02	3.90E+02	4.07E+02	3.94E+02

the fig it is known that the B H F has no effect on the max vonmises stresses. Since its max value is observed at the die corner. Same is evident for maximum plastic strain in fig (6.5). The vonmises stress and plastic strain may be compared at side walls from fig. (6.6) to it is evident that max plastic strain decreases with the die radius and increases further. So there is an optimum die radius where plastic strain for a given BHF is minimum. The same trend is observed in max vonmises stress (fig. 6.7).

Table 6.5: variation of plastic strain with Blank Holding Force at different Coefficient of friction

		Coefficient of friction				
		0.01	0.045	0.06	0.13	0.15
Blank holding force	10250	0.996	0.962	1.103	1.042	1.018
	10500	0.965	1.059	1.038	1.026	1.054
	10750	1.043	1.051	1.037	1.035	1.016
	11000	0.9771	1.009	1.013	1.02	1.06
	11250	1.032	1.013	1.019	1.018	0.9897
	11500	0.961	0.9649	0.9975	1.029	1.057
	11671	0.9849	0.9442	0.952	1.003	1.029
	11750	0.9708	1.029	1.007	0.9989	1.016
	12000	1.066	0.9751	0.9696	1.009	0.9886

C

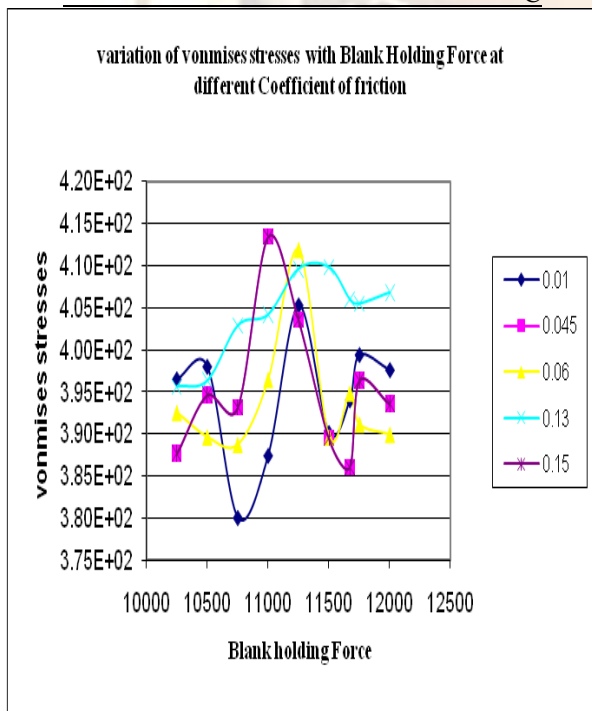


Fig 6.4: variation of vonmises stresses with Blank Holding Force at Different Coefficient of friction

From fig (6.4) it is observed that the max vonmises stress is occurring at the die corner. From

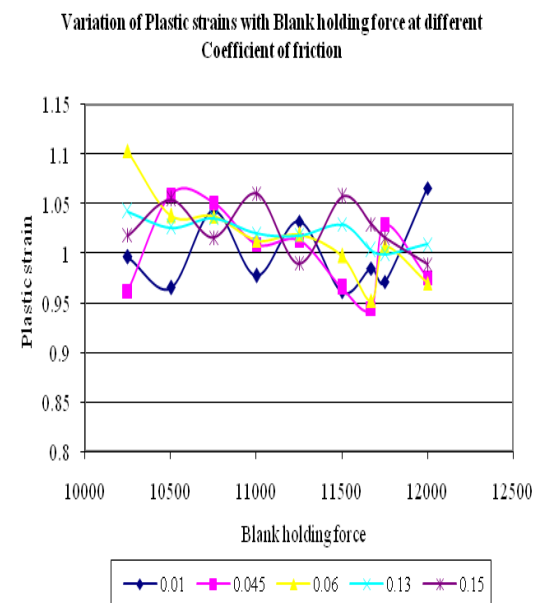


Fig 6.5: variation of plastic strain with Blank Holding Force at Different Coefficient of friction.

Table 6.6 variation of vonmises stresses with Blank Holding Force at Different Die radius

Blank holding force	Die radius				
	2	3	4	5	6
10000	413.8	412	391.3	395	386.8
10250	412	413.4	395.5	385.3	386.4
10500	419.4	407.8	392	397.1	388.4
10750	423.7	414.4	388.9	392.9	390.1
11000	418.9	416.4	391.9	390.1	389.2
11250	427.4	411.5	395.9	397.9	389.7
11500	421.4	411.5	392	389.5	393.2
11671	418.8	409.7	391.4	396.4	389.7
11750	420.7	405.9	400.6	395.7	393.4
12000	419.3	406.8	390.3	390.8	386.4

Table 6.7: variation of plastic strain with Blank Holding Force at Die radius

Blank holding force	Die radius				
	2	3	4	5	6
10000	1.018	1.029	0.987	0.9157	1.092
10250	1.101	1.018	0.9841	0.9506	1.042
10500	1.067	1.054	1	0.9358	1.025
10750	1.126	1.018	0.9514	0.9622	1.069
11000	1.04	1.06	0.9561	0.9392	1.094
11250	1.148	0.9897	0.9671	0.9449	1.091
11500	1.099	1.057	1	0.997	1.062
11671	1.061	1.029	1.076	1.06	1.04
11750	1.082	1.036	1.002	1.007	1.06
12000	1.091	0.9886	1.059	1.059	1.149

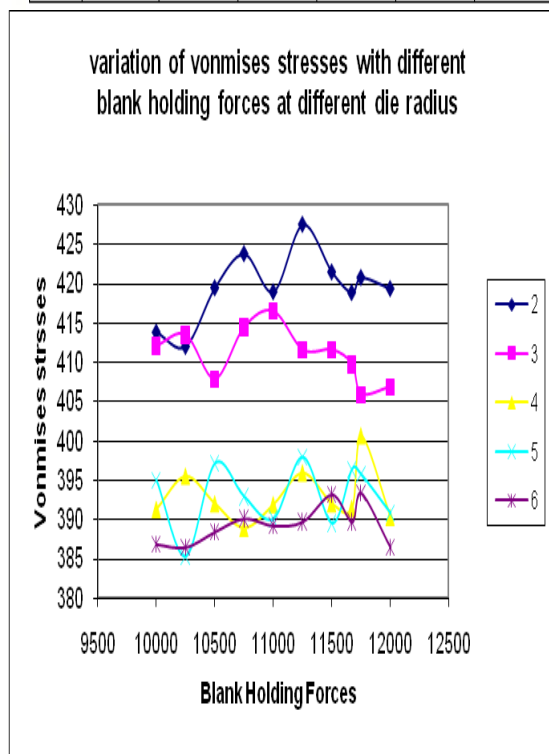


Fig 6.6: variation of vonmises stresses with Blank Holding Force at Different die radius

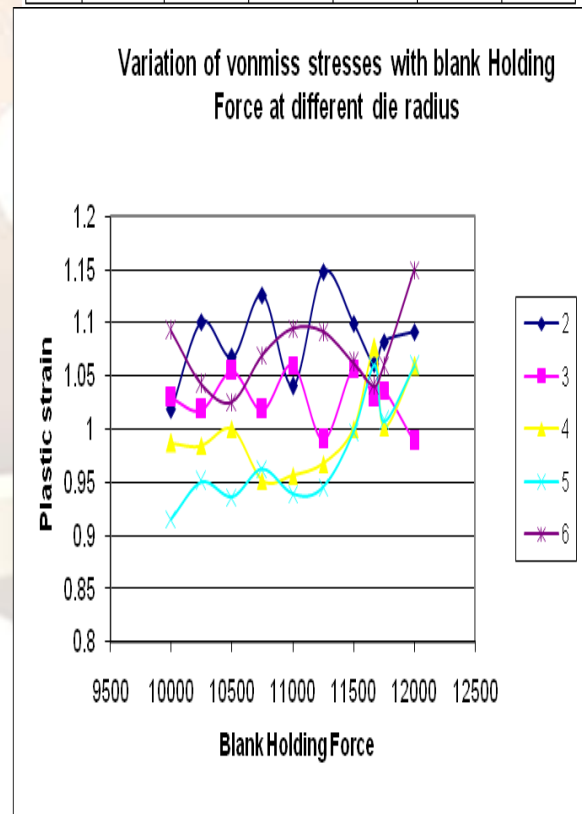


Fig 6.7: variation of plastic strain with Blank Holding Force at Die radius

VII. CONCLUSION

The conclusion of thesis work are enumerated and presented as shown.

- For a given set of punch die and working conditions there exists an optimum blank holding force which prevents the wrinkles and at same from the stresses induced in the cup is minimum.
- Blank holding force decreases with increase of coefficient of friction for a small range of coefficient of friction and a linear relation exists.
- With the increase of die radius up to a certain value Optimum BHF drastically reduces beyond that it remains constant.

There will be an optimum die radius where max plastic strain and max vonmises are minimum.

sheet metal forming processes; theory verification and application. Proceedings of a symposium held by . The Materials Society,1985.p.143-59.

REFERENCES

- [1] Langerak, 1999a .
- [2] Haar R. ter, 'Friction in sheet metal forming: the influence of (local) contact conditions and deformation', Ph.D. Thesis, University of Twente, Enschede, ISBN 90-9009296X, 1996.
- [3] Vreede, 1992] Vreede P.T., 'A finite element method for simulations of 3-dimensional sheet metal forming', Ph.D. Thesis, University of Twente, Enschede, ISBN 90-90047549, 1992).
- [4] Vegter H., Y. An, H.H. Pijlman, J. Huétink, 'Advanced mechanical testing on aluminium alloys and low carbon steels forth sheet forming', Proceedings of the 4th International Conference on Numerical Simulations of 3-D Sheet Metal Forming Processes, J.C. Gelin & P. Picard (eds.), Besançon, vol. 1, p. 3-8, 1999.
- [5] Wang N-M, Budiansky B. Analysis of sheet metal stamping by a finite element method. Journal of Applied Mechanics, ASME Transactions 1978;45:73-82.
- [6] Budiansky B. Notes on nonlinear shell theory. Journal of Applied Mechanics 1968;35:393-401.
- [7] Hughes TJR, Liu WK. Nonlinear finite element analysis of shells: Part I. Three dimensional shells. Computer Methods in Applied Mechanics and Engineering 1981; 26:331-62.
- [8] Belytschko T.Stolarski H.Carpenter N.A C triangular plate element with one-point quadrature. International Journal for Numerical Methods in Engineering 1984;20:787-802.
- [9] Onate E. Zienkiewicz OC A viscous formulation for the analysis of thin sheet metal forming. Internations Journal of Mechanical Sciences 1983;25(5):305-35.
- [10] Stoughton T M. Finite Element Modeling of 1008 AK Steel stretched over a rectangular punch with bending effects In: Wang NM, Tang SC , editors. Computer modeling of